$Ti_3C_2T_x$ Solid Lubricant Coatings in Rolling Bearings with Remarkable Performance beyond State-of-the-Art Materials

Max Marian [1, a*], Klara Feile [1, b], Benedict Rothammer [1, c], Marcel Bartz [1, d], Sandro Wartzack [1, e], Armin Seynstahl [2, f], Stephan Tremmel [2, g], Sebastian Krauß [3, h], Benoit Merle [3, i], Thomas Böhm [4, j], Bo Wang [5, k], Brian C. Wyatt [6, l], Babak Anasori [6, m] and Andreas Rosenkranz [7, n*]

[1] Engineering Design, Friedrich-Alexander-University Erlangen-Nuremberg (FAU), Erlangen, Germany
[2] Engineering Design and CAD, University of Bayreuth, Bayreuth, Germany
[3] Materials Science & Engineering, Institute I, Interdisciplinary Center for Nanostructured Films (IZNF), Friedrich-Alexander-University Erlangen-Nuremberg (FAU), Erlangen, Germany
[4] Forschungszentrum Jülich GmbH, Helmholtz-Institute Erlangen-Nürnberg for Renewable Energy, Erlangen, Germany
[5] Key Laboratory of Marine New Materials and Related Technology, Zhejiang Key Laboratory of Marine Materials and Protection Technology, Ningbo Institute of Material Technology & Engineering, Chinese Academy of Sciences, Ningbo, People's Republic of China
[6] Department of Mechanical and Energy Engineering, and Integrated Nanosystems Development Institute, Purdue School of Engineering and Technology, Indiana University-Purdue University Indianapolis, USA
[7] Department of Chemical Engineering, Biotechnology and Materials (FCFM), Universidad de Chile, Santiago, Chile

[a] marian@mfk.fau.de, [b] klara.feile@fau.de, [c] rothammer@mfk.fau.de, [d] bartz@mfk.fau.de, [e] wartzack@mfk.fau.de, [f] armin.seynstahl@uni-bayreuth.de, [g] stephan.tremmel@uni-bayreuth.de, [h] sebastian.s.krauss@fau.de, [i] benoit.merle@fau.de, [j] t.boehm@fz-juelich.de, [k] wangb@nimte.ac.cn, [l] bcwyatt@iu.edu, [m] banasori@iupui.edu, [n] arosenkranz@ing.uchile.cl

* Corresponding authors

Abstract

Two-dimensional (2D) transition metal carbides, nitrides, and carbonitrides, known as MXenes, are a growing class of 2D materials, which offer great solid lubrication ability for low friction applications due to their weakly bonded multi-layer structure and tribo-layer formation with self-lubricating characteristics. To date, most studies have assessed their tribological response in basic laboratory tests. However, these tests do not adequately reflect the complex geometries, kinematics, and stresses present in machine components. Here, we aim at bridging this gap through assessment of the friction and wear performance of multi-layer $Ti_3C_2T_x$ MXene solid lubricant coatings used in rolling bearings. MXenes' tribological response is compared with state-of-the art solid lubricant coatings, which include molybdenum disulfide (MoS_2), tungsten-doped hydrogenated amorphous carbon (a-C:H:W), and hydrogen-free, more graphite-like amorphous carbon (a-C). Multi-layer $Ti_3C_2T_x$ MXene coatings reduce wear on the bearing washers by up to 94 %, which can be attributed to the transfer of the lubricious MXene nano-sheets to secondary tribo-contacts of the bearing. While the frictional torque of all solid lubricant coatings is similar during steady-operation, the MXene-coated bearings extend the service life by 30 % and 55 % compared to MoS_2 and DLC, respectively. This

contribution demonstrates the ability of MXene solid lubricant coatings to outperform state-of-the-art solid lubricants in dry-running machine components such as rolling bearings.

Keywords

2D materials; MXenes; MoS_2; DLC; solid lubrication; rolling bearings

1. Introduction

MXenes, an emerging class of 2D nanomaterials of early transition metal carbides, nitrides, and carbonitrides, have gained notable attention in the scientific community due to their outstanding material's performance [1–3]. MXenes are denoted by the general formula of $M_{n+1}X_nT_x$ (n = 1 to 4), for which M stands for n + 1 layers of early transition metal from groups 3 - 5 in the 3d - 5d block, X represents n layers of carbon, nitrogen, or mixtures of both which interleave the layers of M, and T_x represents the variety of surface terminations [4]. Compared to graphene and its derivates, MXenes exhibit numerous similarities such as their 2D character, strong in-plane bonding characteristics, and high surface-to-volume ratios [5]. In contrast to other state-of-the-art 2D nanomaterials, MXenes offer enhanced interlayer interactions, which are not only based on van der Waals forces, but also include electrostatic and intermolecular interactions due to functional surface groups [6]. Moreover, MXenes allow for property tuning through the use of different early transition metals or by adjusting the ratio between carbon and nitrogen, which gives them an inherent chemical diversity [5,7]. Their structural, chemical and compositional diversity together with their strong intralayer primary bonding and relatively weaker interlayer secondary bonding characteristics make MXenes promising 2D nano-materials for mechanical and tribological applications [5,8].

With regards to machine components like rolling bearings, which are representative for highly stressed and high volume machine elements, solid lubricant coatings are utilized when these systems cannot be lubricated with conventional oils or greases due to severe environmental conditions. This comprises very high and low temperatures, vacuum, radiation, or due to strict requirements regarding cleanliness, hygiene, and environmental friendliness [9,10]. In the context of solid lubricants, soft metals, polymers, transition metal dichalcogenides (TMDs), and carbon-based materials are frequently used [11]. Thereby, soft metals and/or polymers feature some limitations particularly in the case of pronounced sliding or at elevated pressures and temperatures [12,13]. TMDs and in particular molybdenum disulfide (MoS_2) exhibit excellent sliding properties over a wide range of contact conditions, loads, and temperatures because of their hexagonal crystal structure and the ease of basal plane slip [14]. Due to the tendency to oxidize under atmospheric conditions and the significant influence of humidity [15,16], TMDs applications are mainly in dry and vacuum environments. In this respect, MoS_2 coatings have also been successfully employed for rolling bearing components [17,18]. Graphite, graphene, and their derivatives also offer good solid lubrication properties owing to the easy-to-shear ability of its densely packed and atomically smooth surface, especially but not limited to moist and ambient environments [19]. Nevertheless, there are only few application-oriented studies on highly loaded rolling-sliding contacts as encountered in rolling bearings [20]. In addition, amorphous or diamond-like carbon (DLC) coatings with high hardness, low wear rates and low friction coefficients are promising alternatives [21]. These coatings can be doped with metals or lightweight elements to accommodate relatively large residual compressive stresses and prevent delamination [22], and thus have found several applications in commercial products. Like other solid lubricants, their tribological properties exhibit a dependence on the operating conditions and environment, whereby hydrogen-free DLC coatings perform well in humid air, and hydrogenated coatings perform better in dry or inert gas environments [11]. Amorphous carbon coatings have also been successfully applied to highly loaded contacts in rolling element bearings [23–25]. One of the major advantages of MoS_2 or DLC coatings is that the components do not have to be geometrically modified compared to the operation without solid lubricant coatings, since the involved coating thicknesses do not impair the function.

Although these aforementioned materials have been extensively studied in previous publications, the fundamental tribological behavior of MXenes has recently come into the focus of the tribological community [5,26,27]. Initially, MXenes were studied as lubricant additives in paraffin [28], poly-(alpha)-olefin [29], and other base oils [30,31] to optimize the resulting friction and wear performance. Furthermore, MXenes have been used in metal [32,33] and polymer [34,35] matrix composites as the reinforcement phase. In particular, the use of MXenes as solid lubricant coatings demonstrated promising results at the nano- and macroscopic scales for enhancing friction and wear behavior [36–40]. Besides the fundamental dependencies of friction and wear on contact pressure and relative humidity [41], the solid lubrication ability of hybrid coatings (combination of MXenes and graphene/graphene oxide or MXenes and nanodiamonds) has been investigated [42–44]. Very recently, 100-nm-thick multi-layer MXene coatings deposited by electro-spraying onto stainless steel have verified their outstanding wear resistance and ability to outperform state-of-the-art 2D materials with regard to their durability and longevity [45]. The improved wear performance was traced back to the formation of a beneficial tribo-layer consisting of amorphous and nanocrystalline iron oxide intermixed with thermally and structurally degraded MXenes. This observation aligns well with the good wear performance of hybrid MXene coatings.

Until now, the tribological studies on MXenes have mainly focused on titanium-based MXenes (mainly $Ti_3C_2T_x$ nano-sheets), and the fundamental effects/mechanisms were explored by laboratory model tests under pure sliding motion. When this knowledge is transferred to macro-scale and application-oriented conditions with more complex geometries, kinematics and stresses, the underlying mechanisms are yet to be explored [46]. Recently, Marian *et al.* [47] applied MXene nano-sheets as solid lubricants to highly loaded rolling-sliding contacts of machine elements. In component level testing, an up to 3.2-fold friction reduction, a decrease in the cumulative linear wear by 2.9 times, and an extension of service life by a factor of 2.1 were observed for $Ti_3C_2T_x$-coated thrust ball bearings, compared to uncoated references. This indicates the potential of MXenes to lubricate dry-running machine elements effectively and efficiently.

Although various solid lubricant coating systems with specific advantages and limitations have been used for dry-running machine components, the development and qualification of novel MXenes as solid lubricant coatings with comparison to other state-of-the art 2D materials is currently scarce. Apart from our own previous study [47], MXenes' tribological performance has been mainly assessed by fundamental laboratory tests using simplified test rigs, which do not adequately represent the conditions of highly loaded sliding-rolling contacts and the interaction of multiple components in machine elements such as rolling bearings. This study aims at elucidating the friction and wear performance of multi-layer $Ti_3C_2T_x$ solid lubricant coatings in rolling bearings working under realistic conditions. The tribological performance of the MXene coatings is compared with the performance of state-of-the art solid lubricant coatings, namely DLC and MoS_2.

2. Materials and Methods

2.1. Specimens

Due to the large sliding and spinning friction portions as well as the facilitated possibility for coating deposition, commercially available 51201 thrust ball bearing washers specified in ISO 104 [48] were used. The complete axial rolling bearing consisted of shaft washer, ball cage assembly (rolling elements + sheet metal cage) and housing washer. The rolling elements as well as the bearing washers were made of 100Cr6 (1.3505, AISI 52100) bearing steel.

2.2. Coating deposition

To evaluate their solid lubrication ability, $Ti_3C_2T_x$, MoS_2 and two DLC coatings were deposited on the bearing washer raceways. Prior to deposition, the bearing components were ultrasonically cleaned in acetone and isopropyl alcohol for 10 minutes each (Sonorex Super RK 255H 160 W 35 Hz, Bandelin electronic GmbH & Co. KG, Berlin, Germany) and subsequently blow-dried with nitrogen.

2.2.1. $Ti_3C_2T_x$ coating

The synthesis of multi-layer $Ti_3C_2T_x$ nano-sheets made use of 10 g of Ti_3AlC_2 powder (Forsman Scientific Co. Ltd., Beijing, China), which was immersed in 100 mL of a 40 % HF solution. The solution was stirred at room temperature for about one day prior to a washing and centrifugation treatment. After one centrifugation step, the supernatant was poured out and fresh deionized water was added, until reaching a pH of about 6. Subsequently, the final MXenes were filtered under vacuum and freeze-dried at a temperature of −60 °C and pressure of below 30 Pa for 24 hours. The MXenes were then dispersed in acetone (10 mg/mL), stirred (AREX-6 digital heating magnetic stirrer, Velp Scientifica Srl, Usmate, Italy) and ultrasonicated (Sonorex Super RK 255H, 160 W, 35 Hz, Bandelin electronic GmbH & Co. KG, Berlin, Germany) at room temperature for 10 minutes each to ensure good dispersion. Prior to testing, 300 µL of the dispersion were drop-casted (1000 series gastight 81420, Hamilton Germany GmbH, Gräfelfing, Germany) onto each bearing washer raceway, which yielded the $Ti_3C_2T_x$ coating after solvent evaporation. In contrast to previous studies [47], no MXenes were applied to the ball cage assembly to ensure better comparability with the MoS_2- and DLC-coated bearings.

2.2.2. DLC coatings

The DLC coatings were fabricated using an industrial-scale coating plant (TT 300 K4, H-O-T Härte und Oberflächentechnik GmbH & Co. KG, Nuremberg, Germany) for physical vapor deposition (PVD). Two coating systems with tungsten-containing, hydrogenated amorphous carbon (a-C:H:W) and hydrogen-free amorphous carbon (a-C) as tribologically effective functional layers were deposited under 2-fold rotation. These were selected due to their promising tribological behavior under dry conditions [49,50] and in rolling bearings [23,24,51]. The chamber was initially evacuated to a base pressure of 2.4×10^{-4} Pa and heated to 250 °C for 40 minutes. Subsequently, the samples were argon-ion (Ar^+) plasma etched for 40 minutes using an argon (Ar) flow of 500 sccm and a bipolar pulsed bias voltage of −500 V (pulse frequency 40 kHz, reverse recovery time 5 µs).

The same cleaning procedure was carried out for the powder metallurgical chromium (Cr, purity 99.998 %), tungsten carbide (WC, purity 99.9 %), and graphite (C, purity 99.998 %) targets (267.5 × 170 mm). First, a thin Cr adhesion layer was applied and transferred to a WC support layer. Efforts were made to achieve graded transitions to the substrate and between the individual layers by continuously adjusting the process parameters (please refer to Table 1). The a-C:H:W and a-C layers were subsequently deposited by reactive and non-reactive PVD through unbalanced magnetron UBM sputtering under argon-acetylene (Ar-C_2H_2) and pure Ar atmosphere, respectively. In contrast to the a-C:H:W layer, the a-C layer had to be applied in two steps. The first step was to lower the tungsten and hydrogen content by gradually reducing the cathode power and reducing the C_2H_2 flow (purity 99.5 %). Secondly, the coating process was interrupted to replace the Cr with the C target due to the coating plant configuration. Subsequently, the chamber was re-evacuated and heated to 100 °C for 40 minutes, followed by Ar^+-ion plasma etching for 5 minutes. Thereafter, the a-C functional layer was deposited with a gradual increase in bias voltage.

Table 1. Cathode, process and reactive gas parameters for the deposition of the a-C:H:W, a-C, and MoS_2 coatings. The dashed line indicates the interruption in the deposition process.

coating	layer	power	pulse frequency	reverse recovery time	duration	bias voltage	chamber temperature	Ar flow	C_2H_2 flow
a-C:H:W	Cr	5.0 kW	40 kHz	5 µs	240 s	−100 V	160 °C	180 sccm	-
	CrWC	5.0 | 0.3 ↗ 1.2 kW	40 kHz	5 µs	960 s	−100 V	150 °C	180 sccm	-
	WC	1.2 kW	40 kHz	5 µs	1080 s	−100 V	130 °C	195 sccm	-
	a-C:H:W	1.5 kW	40 kHz	5 µs	5400 s	0 V	100 °C	90 sccm	25 sccm
a-C	Cr	5.0 kW	40 kHz	5 µs	240 s	−100 V	160 °C	180 sccm	-
	CrWC	5.0 | 0.3 ↗ 1.2 kW	40 kHz	5 µs	960 s	−100 V	150 °C	180 sccm	-
	WC	1.2 kW	40 kHz	5 µs	1080 s	−100 V	130 °C	195 sccm	-
	a-C:H:W	1.5 kW	40 kHz	5 µs	5400 s	−50 V	100 °C	90 sccm	25 sccm
	a-C	2.0 kW	75 kHz	3 µs	7205 s	-30 ↗ -170 V	100 °C	90 sccm	-
MoS_2	MoS_2	2.0 kW	70 kHz	4 µs	7200 s	0 V	50 °C	120 sccm	-

2.2.3. MoS_2 coating

Under 3-fold rotation, the substrates were MoS_2-coated using the same coating plant as for DLC and a hot-pressed powder target (purity 99.5 %, 260 × 163 mm). Prior to deposition, the chamber was evacuated to achieve an initial pressure of 2.5 × 10^{-3} Pa and was heated to 50 °C. Subsequently, the specimens' surfaces were cleaned and activated by Ar^{+}-ion plasma etching with the same procedure as described in section 2.2. Furthermore, cathode sputtering was performed for 3 minutes with closed shutters to remove impurities and the thin oxide layer from the target. Afterwards, the MoS_2 coating was deposited by PVD through UBM sputtering under Ar atmosphere without applying any additional adhesion layer. The deposition parameters were selected based upon [16,52,53] and are summarized in Table 1.

2.3. Coating characterization

The thickness and structure of the as-deposited coatings were characterized utilizing a focused ion beam scanning electron microscope (FIB-SEM; NanoLab 600i, FEI Thermo Fisher, Hillsboro, OR, USA). For electron imaging, secondary electron contrast, an acceleration voltage of 5 kV, an electron current of 0.69 nA, and a working distance of 4 mm were used. Cross-sections of the coatings were fabricated by FIB milling. At first, a protective platinum (Pt) layer was locally deposited onto the samples to avoid FIB damage [54]. Decreasing ion beam currents of 2.5, 0.79, and 0.23 nA were subsequently used for sequentially milling the coatings. After final ion polishing, the cross sections were investigated by SEM with a tilting angle of 52°. Furthermore, the stoichiometry of the MoS_2 coating was investigated via energy-dispersive X-ray spectroscopy (EDX; Oxford Instruments plc, Abingdon, UK) using an acceleration voltage of 20 kV and an electron current of 2.7 nA. The spectra were recorded while scanning an area of approx. 10 × 6 μm^2. In addition, EDX line scans in the FIB-milled cross sections were recorded to reveal the coatings' architectures. Moreover, digital light microscopic images and Raman spectra were acquired (WITec alpha 300R, WITec Wissenschaftliche Instrumente und Technologie GmbH, Ulm, Germany) with excitation at 457 nm and a laser power of 0.15 mW. The spectra were integrated for 5 s with 5 accumulations and background-corrected (shape-based algorithm, WITec Project FIVE+). Finally, averaged spectra from different spots on the samples were obtained after intensity normalization.

2.4. Tribological testing

Tribological tests were performed on a TRM1000 tribometer (Wazau Mess- + Prüfsysteme GmbH, Berlin, Germany) with modified set-up under laboratory ambient conditions [47]. Thereby, the housing washer was driven with 1000 min^{-1} (10 % of the catalog speed limit), while the shaft washer was fixed and cardanically mounted for uniform loading. A normal force of 130 N (15 % of the catalog axial fatigue limiting load) was applied via weights on the stationary mounting, providing an initial Hertzian pressure of 800 MPa. The measurements, especially the resulting frictional torque, were recorded at a frequency of 10 Hz. Similar to [47], a frictional torque of 1.3 Nm was defined as termination criterion of the tests. Three experiments were performed for each bearing type (uncoated references, a-C:H:W-, a-C-, MoS_2- and MXene-coated) with new samples. The measurements were analyzed for a distinct rise in the frictional torque, which indicated incipient coating failure, thus defining the end of the service life. Since each volume element on the bearing washers is rolled over several times per revolution, the number of endured overrollings was used as a criterion for comparison. Additionally, the frictional torque during service life and the gravimetric wear were analyzed. Regarding the latter, the bearings were weighed prior to and after tribological testing (ALS-A/ALJ-A, Kern & Sohn GmbH, Balingen-Frommern, Germany).

3. Results and Discussion

3.1. Coating properties

SEM micrographs of the as-deposited coatings (plane-view and FIB-milled cross-sections), averaged EDX line scans and the averaged Raman spectra are depicted in Figure 1. The thicknesses of the a-C:H:W and the a-C coatings were measured to be around 1.5 and 1.0 µm, respectively (Figure 1b, f). The multilayer character with the WC inter- and the Cr adhesion layers can also be seen from the EDX line scans (Figure 1c, g). The cauliflower-like topographies of both coatings pointed towards a DLC-typical and fine columnar growth [55] (Figure 1a, e). The Raman spectra

(Figure 1d, h) featured two distinct peaks around 1340 and 1555 cm^{-1}, which are characteristic for the D- and G-bands of DLC coatings [56,57]. For the a-C:H:W coating (Figure 1d), the ratio between the peak intensities of the D- and G-bands, which is an indicator for the sp^2 and sp^3 content [58], aligns well with hydrogenated amorphous carbon [56]. The spectrum of the a-C coating (Figure 1h) suggested a more graphite-like carbon (GLC) [50,59]. Detailed insights in the mechanical and chemical characterization of similar coatings can be found elsewhere [49,50].

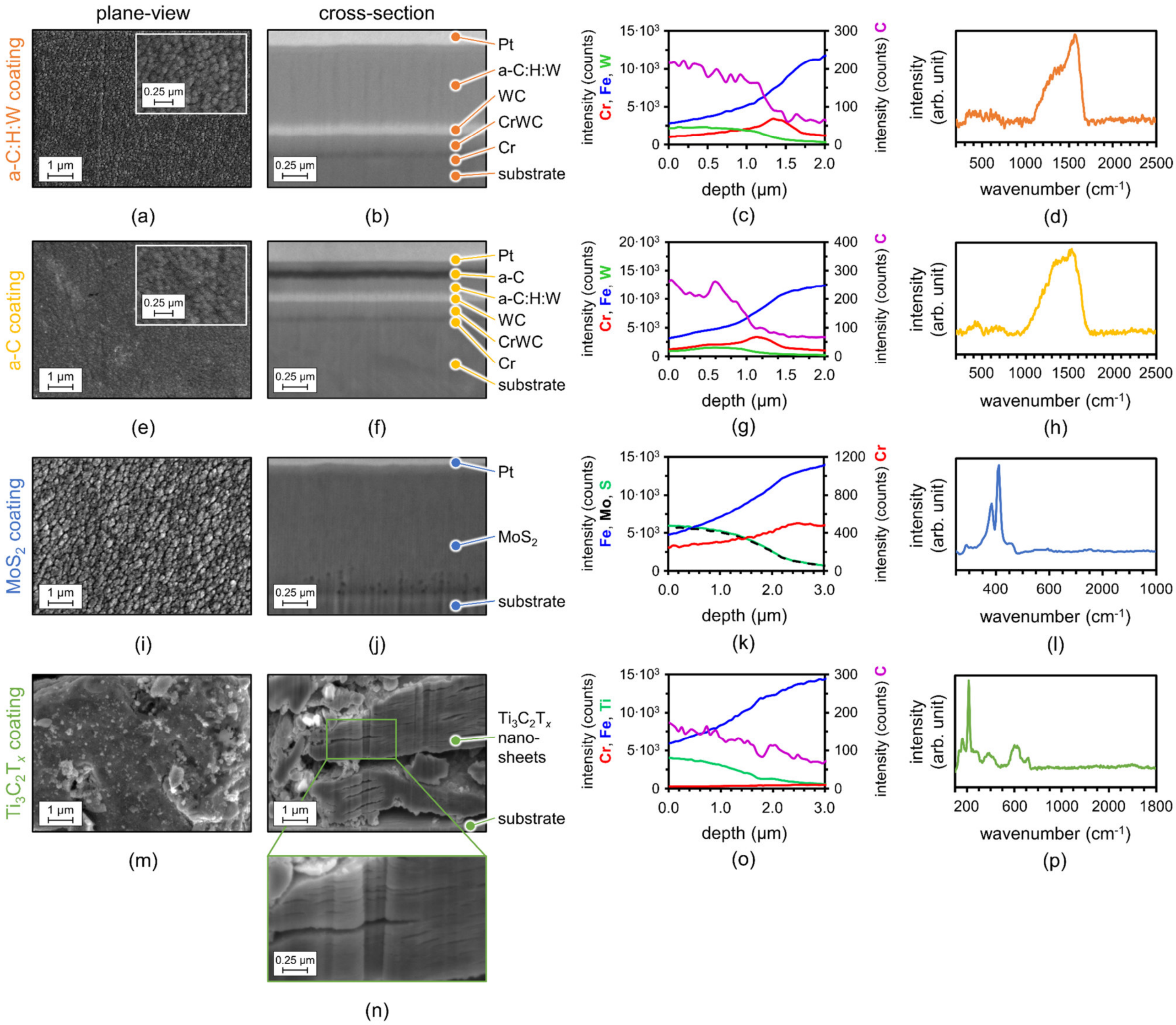

Figure 1. SEM-micrographs and FIB cross-sections of the as-deposited (a, b) a-C:H:W, (e, f) a-C, (i, j) MoS_2 and (m, n) $Ti_3C_2T_x$ coatings. Pt corresponds to a protection layer deposited during FIB processing. Averaged EDX line scans of the as-deposited (c) a-C:H:W, (g) a-C, (k) MoS_2 and (o) $Ti_3C_2T_x$ coatings. Averaged Raman spectra of the as-deposited (d) a-C:H:W, (h) a-C, (l) MoS_2 and (p) $Ti_3C_2T_x$ coatings.

The MoS_2 coating featured a thickness of about 1.3 µm, was slightly deficient in sulfur with a S/Mo-ratio of about 1.82 according to EDX analysis (Figure 1k), and showed a dendritic and porous growth (Figure 1i, j). This could be attributed to the 3-fold substrate rotation during deposition [52]. The Raman spectrum of the MoS_2 sample (Figure 1l) showed pronounced double peaks at 380 and 407 cm^{-1}, which can be attributed to first order E^1_{2g} and A_{1g} modes of hexagonal MoS_2 [60–64]. Further peaks were observed at 286 and 453 cm^{-1}, corresponding to E_{1g} and 2LA(M) modes [60,61,65,66]. A more detailed characterization of similar MoS_2 coatings can be found in [52].

The MXene coating mainly consisted of multi-layered $Ti_3C_2T_x$ nano-sheets (Figure 1m, o), for which the well-known accordion-like structure was observed in the cross-section images (Figure 1n) [41]. The Raman spectrum (Figure 1p) indicated distinct peaks around 160, 220, and 707 cm^{-1} as well as wider peaks around 285, 375, and 600 cm^{-1}. The first peak may be correlated with in-plane $Ti_3C_2T_x$ vibrations or minor contributions originating from anatase TiO_2, which may be correlated with smaller particles observed in SEM (bright submicron particles in Figure 1m) and minor surface oxidation. However, these particles are expected to play a minor role for the tribological experiments. All other peaks can clearly be assigned to vibrations originating from $Ti_3C_2O_2$, $Ti_3C_2F_2$ and $Ti_3C_2(OH)_2$ [67–70]. The occurrence of -O, -F and -(OH) groups can be explained by the MXenes' synthesis involving selective etching with HF and the replacement of aluminum with respective surface terminations [41,47]. For a more in-depth characterization of the MXene coating by high-resolution transmission electron microscopy, X-Ray photoelectron spectroscopy, or X-Ray diffraction, the interested reader is referred to our previous studies [37,40–42,47].

The MXene layer thickness could be estimated to be between 2 and 4 µm with thickness deviations over the raceway, which can be traced back to the size of the stacked MXenes as well as the solvent evaporation during drop-casting, and the raceway's curvature. This resulted in the layer thickness at the inner and outer edge of the raceway being slightly thinner than the thickness in the center. Due to the variation in thicknesses and the less dense character of the $Ti_3C_2T_x$ coating compared to the MoS_2 and DLC coatings, a comparison of the usable lubricant volume purely based on the coating thickness may not be conclusive. The estimation of the available solid lubricant mass allows for a fairer comparison. In case of the MXene coating, the mass can be estimated based on the known drop-casting conditions (300 µL at a concentration of 10 mg/mL). For the MoS_2 and DLC coatings, the available masses can be approximated based on the raceway geometry of the 51201 thrust ball bearing washers [48] (~ 4.5 cm^2), the measured thickness, and density data from literature (5.1 g/cm^3 for MoS_2 and 2.6 g/cm^3 for DLC) [14,71–73]. The estimated available masses for MXene and MoS_2 coatings are comparable with about 3 mg, while a-C:H:W and a-C were at about half of that (1.6 mg for a-C:H:W and 1.1 mg for a-C).

3.2. Friction, wear, and service life

Representative evolutions of the frictional torque versus overrollings are presented in Figure 2 for the uncoated reference (Figure 2a) as well as the a-C:H:W-, a-C-, MoS_2-, and MXene-coated bearings (Figure 2b-e). All tested specimens initially exhibited a rather low and constant frictional torque. After a certain test duration, it increased sharply and leveled off with pronounced fluctuations. Ultimately, it reached the switch-off threshold due to severe cage failure as well as clamping, fretting, and overheating of the rolling elements, which we considered to be catastrophic failure [47]. We defined the first pronounced increase in friction exceeding 0.5 Nm as the end of service life. This corresponds to the end of the bearing's usability due to high friction, non-smooth operation and incipient wear. The mean number of overrollings as well as the frictional torque until the end of the service life were compared in Figure 2f, g and Table 2 for the different coating types. Moreover, the mean gravimetric wear loss after tribological testing is summarized in Table 2 and depicted in Figure 2 for (h) the shaft and (i) the housing washer as well as (j) the ball cage assembly. Since the total running time of each individual bearing was different, these values were normalized to the number of overrollings to enable a fair comparison. Digital optical light microscopic images of worn surfaces of the MXene-coated washer raceway (a), the corresponding ball (b) and cage (c) with measurement positions for Raman spectroscopy as well as averaged spectra (d) are displayed in Figure 3.

Table 2. Averaged number of overrollings and frictional torque until end of service life as well as averaged gravimetric wear per overrolling of the shaft washer, housing washer, and ball cage assembly, respectively.

	uncoated reference	**a-C:H:W**	**a-C**	**MoS_2**	**$Ti_3C_2T_x$**
averaged overrollings until end of service life	3.17 x 10^5	5.58 x 10^5	5.58 x 10^5	6.66 x 10^5	8.67 x 10^5
averaged frictional torque until end of service life	0.20 Nm	0,15 Nm	0,14 Nm	0,14 Nm	0,15 Nm
averaged gravimetric shaft washer wear per overrolling	2.1 x 10^{-4}	7.5 x 10^{-6}	1.1 x 10^{-5}	7.5 x 10^{-5}	1.5 x 10^{-5}
averaged gravimetric housing washer wear per overrolling	1.0 x 10^{-5}	4.9 x 10^{-6}	4.4 x 10^{-6}	5.0 x 10^{-6}	4.0 x 10^{-6}
averaged gravimetric cage assembly wear per overrolling	2.1 x 10^{-4}	3.3 x 10^{-4}	3.3 x 10^{-4}	2.1 x 10^{-4}	2.1 x 10^{-4}

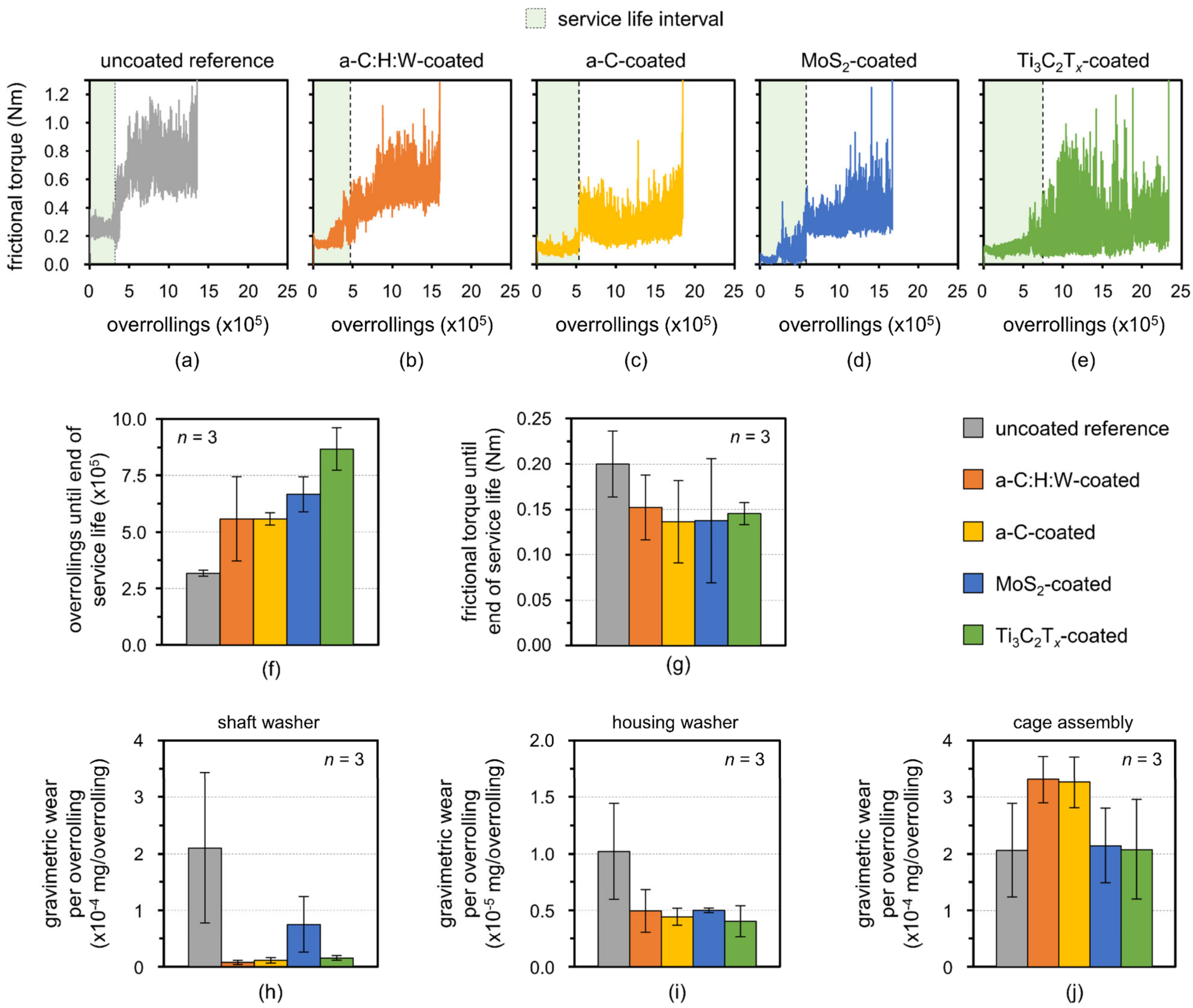

Figure 2. Frictional torque versus overrollings for representative tests with (a) uncoated reference, (b) a-C:H:W-, (c) a-C-, (d) MoS_2- and (e) $Ti_3C_2T_x$-coated bearings (representative graphs). The service life interval is indicated by the dashed line and the area highlighted in light green. (f) Averaged number of overrollings and (g) averaged frictional torque until end of service life. Averaged gravimetric wear per overrolling of (h) shaft washer, (i) housing washer and (j) cage assembly. Data show mean ± standard deviation for *n* = 3.

The uncoated reference (Figure 2a) started with the largest frictional torque around 0.2 Nm (Table 2, Figure 2g, grey) and its service live ended comparatively early after an average of 3.2×10^5 overrollings (Table 2, Figure 2f, grey). This was due to the lack of a damping lubricant and the associated orbital and tilting movements of the ball guided cage with substantial stresses building up between the rolling elements and the cage pockets [47]. Accordingly, the frictional torque became increasingly unstable, reaching values between 0.6 and 1.1 Nm (Figure 2a) until catastrophic failure occurred. Thereby, the bearing washers also showed considerable signs of wear, which was also reflected by the comparatively high gravimetric loss of mass (Table 2, Figure 2h and i, grey).

Bearings coated with solid lubricants demonstrated a slightly lower initial friction level (Figure 2b-e), which were between 0.13 and 0.15 Nm on average (Table 2, Figure 2g), without significant differences between the various coating types when taking into account the standard deviations. All coatings at least ~ doubled the service life of the bearings compared to the uncoated reference (Table 2, Figure 2f). The bearings also failed due to the fatal cage assembly malfunction, making reliable statements regarding gravimetric cage wear (Figure 2j) difficult. However, it could be observed that the wear on the bearing washers was notably reduced by the solid lubricant coatings (Table 2, Figure 2h and i).

The DLC-coated bearings initially showed low frictional torque, which increased to values between 0.4 and 0.8 Nm (a-C:H:W, Figure 2b) as well as 0.15 and 0.6 Nm (a-C, Figure 2c) after the end of service life. The latter was reached after an average of 5.6×10^5 overrollings for both types, representing a 1.8-fold increase compared to the reference (Table 2, Figure 2f, orange and yellow). Regarding wear, a significant wear reduction of about 95 % (shaft washer) and 52 % (housing washer) was verified for both DLC coatings (Table 2, Figure 2h and i, orange and yellow).

In the case of the MoS_2 coating, there was a rise in frictional torque on average after 6.7×10^5 overrollings (end of service life), which represented an enhancement by a factor of 2.1 compared to the uncoated reference (Table 2, Figure 2f, blue). This was comparable to previous results from Vierneusel [74] on undoped and superior to Ti- or Cr-doped MoS_2 coatings with the same tribometer and setup. Afterwards, the bearings still operated at frictional torque levels between 0.2 and 0.6 Nm for some time with stronger fluctuations prior to catastrophic failure (Figure 2d). In terms of wear of the bearing washers, there was a reduction of 64 % (shaft washer) and 51 % (housing washer) compared to the uncoated reference (Table 2, Figure 2h and i, blue).

MXene-coated bearings initially operated at low friction levels, which gradually began to fluctuate more as the service life approached its end but remained at relatively low levels between 0.1 and

0.6 Nm (Figure 2e). The mean service life of 8.7 × 10^5 overrollings exceeded that of the reference by a factor of 2.7 (Table 2, Figure 2f, green). The wear of the bearing washer was reduced by 93 % (shaft washer) and 61 % (housing washer), respectively (Table 2, Figure 2h and i, green). The observed wear reduction was similar to the a-C:H:W and the a-C coatings as well as superior to MoS_2. Considering the deposited masses (see discussion in section 3.1) and the higher density of MXenes as well as MoS_2 compared to DLC, it can be assumed that the total wear volume was also substantially reduced. This indicates that MXenes are a rather clean ("green") solid lubricant. With regard to combining an extended service life with smooth operation and low frictional torques, the more easy-to-shear and less adhering coatings (MXenes, MoS_2, and the more graphite-like a-C) seemed to be particularly suitable due to their potential tribo-film formation and transfer to the counter-bodies. For MoS_2 and GLC, this had previously been reported in literature [14,75–77], but we were not able to verify the respective transfer to the counter bodies for these coatings after fatal bearing failure. In case of the MXene coating, some areas of the bearing raceways were exposed and affected by wear, while other regions were still protected by films of compacted nano-sheets (Figure 3a). Based upon optical micrographs (Figure 3b and c) and the corresponding Raman spectra (Figure 3d), which featured typical MXene peaks at about 222, 290, 380 and 600 cm^{-1}, it becomes evident that lubricious material originating from a tribo-layer was transferred to secondary tribo-contacts of the bearing (particularly the contacts between rolling elements and cage pockets), thus enhancing the friction and wear performance. This mechanism is schematically illustrated in Figure 3e. Based upon our previous studies and the available literature, $Ti_3C_2T_x$ nano-sheets have shown to enable the formation of lubricious tribo-layers consisting of degraded MXenes intermixed with nanocrystalline/amorphous oxide structures (mostly iron oxide from the substrate with some titanium oxide) [45]. These beneficial tribo-layers have been demonstrated to extend the coatings' lifetime, thus notably contributing to their durability and longevity. Regarding the MXenes' degradation, the thermomechanical and cyclic stress during tribological testing may induce structural and chemical changes (reduced number of layers, reduced x-y dimensions, increased defect density, and oxidation) [45]. This was also reflected in changed peak intensities and positions in the Raman spectrum (Figure 3d) compared to the as-deposited coating (Figure 1l). However, the Raman signal after the experiment did not indicate excessive oxidation, which also suggests that the synthesis process did not substantially result in major oxidation of the as-deposited MXenes.

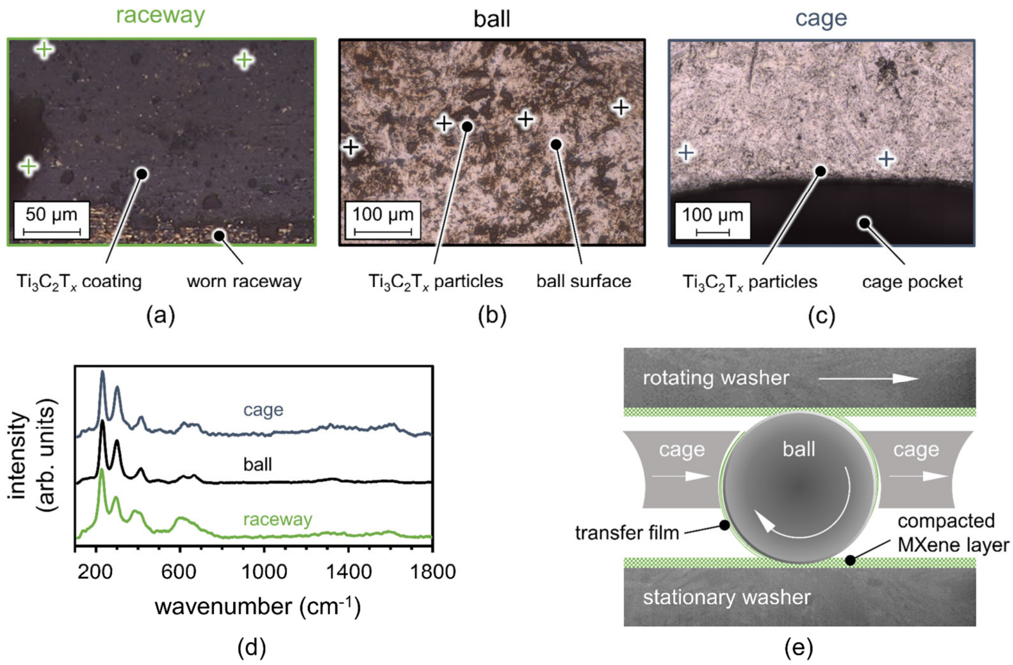

Figure 3. Optical light micrographs (a) raceway, (b) ball and (c) cage of the run MXene-coated bearing as well as (d) averaged Raman spectra. The marks correspond to the positions for Raman measurements. (e) Schematic illustration of the underlying mechanisms based upon compacted MXene nano-sheets and transfer films acting as solid lubricants between primary (ball/raceway) and secondary (ball/cage) rolling bearing contacts.

In general, our results indicate that the service life of the MXene-coated bearing was extended by 30 and 55 % compared to MoS_2 and DLC coating, respectively (Figure 2f). This observation has to be assessed against the background of potential influences regarding different morphologies of the coatings as well as testing and environmental conditions onto the tribological performance of solid lubricants like MoS_2 and DLC [78,79], which, however, equally apply to MXenes [41]. It should be emphasized that MoS_2 and DLC have already been explored and optimized for their usage in rolling bearings over several decades [80,81]. Our experimental finding that MXenes show a comparable or even superior performance underlines their tremendous potential, especially considering the early stage of tribological research. More research effort needs to be dedicated towards the deposition of more uniform MXene coatings with improved interfacial and adhesive properties by utilizing spray coating or electrophoretic deposition [5,45]. However, it should be noted that certain initial wear can be beneficial to initiate the tribo-film formation as well as the respective transfer to the counter bodies, which may lead to ultralow wear in secondary contacts of the machine components [45]. Despite the investigated thrust ball bearings feature several contacts, including lower-loaded secondary sliding contacts between ball and cage and the higher-loaded primary rolling-sliding contacts between ball and raceway, basic model tests under rolling-sliding motion (two-disk tribometer or mini traction machine) are advisable in the future for an improved understanding of the fundamental mechanisms. This also comprises the study of the influence of thermal properties with regard to cooling effects as well as the damping of vibrations. Furthermore, future research work regarding the usage of further MXenes with different stoichiometry or early transition metals [4,7] as well as tailored surface functionalization by making use of their richness in available surface terminations will further boost their tribological performance [5].

4. Conclusions

MXenes have recently shown excellent solid lubrication ability with an enhanced wear performance due to their weakly bonded multi-layer structure and tribofilm formation with self-lubricating character, which is of particular interest for dry-running tribo-systems. This contribution investigated the friction and wear performance of multi-layer $Ti_3C_2T_x$ coatings applied to rolling bearings and compared the tribological performance of MXenes with the performance of state-of-the art solid lubricant coatings including MoS_2, a-C:H:W, and a-C. It was found that MXene coatings reduced wear on the bearing washers by up to 94 % relative to uncoated references, which was comparable to DLC coatings and even superior to MoS_2 coatings. While the frictional torque of all solid lubricants was similar during steady-state operation, the MXene-coated bearings extended the average service life by 30 and 55 % compared to MoS_2 and DLC, respectively. This was traced back to the transfer of lubricious nano-sheets to secondary tribo-contacts of the bearing, particularly between rolling elements and cage pockets, which was verified by Raman spectroscopy. This contribution demonstrated MXenes' general ability to outperform state-of-the-art solid lubricants when applied to dry-running machine components such as rolling bearings.

Conflict of Interest

The authors declare that they have no known competing financial interests or personal relationships that could have appeared to influence the work reported in this manuscript.

Acknowledgments

M. Marian, B. Rothammer, M. Bartz and S. Wartzack greatly acknowledge the continuous support of Friedrich-Alexander-University Erlangen-Nuremberg (FAU), Germany.

Funding

A. Seynstahl, S. Tremmel, S. Krauß and B. Merle acknowledge the financial support by the German Research Foundation (DFG) within the priority program SPP 2074 "Fluid-free lubrication systems with high mechanical loads" (407707942, TR 1043/7-1, ME 4368/7-1). A. Rosenkranz acknowledges the financial support given by ANID-CONICYT within the project Fondecyt 11180121 and the VID of the University of Chile in the framework of U-Inicia UI013/2018. A. Rosenkranz and B. Wang acknowledge the financial support of the Chinese Academy of Sciences President's International Fellowship Initiative (2020VEC0006).

Author Contributions

M. Marian conceived the idea. B. Wang synthesized the $Ti_3C_2T_x$ nano-sheets. B. Rothammer and A. Seynstahl designed and deposited the DLC and MoS_2 coatings. S. Krauß and T. Böhm characterized the as-deposited coatings by SEM, EDX and Raman spectroscopy. K. Feile and M. Marian carried out the experiments and analyzed the data. M. Marian and A. Rosenkranz wrote the manuscript. All authors contributed to the discussion and have reviewed, edited, and approved the final version of the manuscript.

References

[1] M. Naguib, V.N. Mochalin, M.W. Barsoum, Y. Gogotsi, 25th anniversary article: MXenes: a new family of two-dimensional materials, Adv. Mater. Weinheim. 26 (2014) 992–1005. https://doi.org/10.1002/adma.201304138.

[2] B. Anasori, M.R. Lukatskaya, Y. Gogotsi, 2D metal carbides and nitrides (MXenes) for energy storage, Nature Reviews Materials 2 (2017) 16098. https://doi.org/10.1038/natrevmats.2016.98.

[3] M. Naguib, M. Kurtoglu, V. Presser, J. Lu, J. Niu, M. Heon, L. Hultman, Y. Gogotsi, M.W. Barsoum, Two-dimensional nanocrystals produced by exfoliation of Ti3 AlC2, Adv. Mater. Weinheim. 23 (2011) 4248–4253. https://doi.org/10.1002/adma.201102306.

[4] B. Anasori, Y. Gogotsi, 2D Metal Carbides and Nitrides (MXenes): Structure, Properties and Applications, Springer International Publishing; Imprint: Springer, Cham, 2019.

[5] B.C. Wyatt, A. Rosenkranz, B. Anasori, 2D MXenes: Tunable Mechanical and Tribological Properties, Adv. Mater. Weinheim. (2021) e2007973. https://doi.org/10.1002/adma.202007973.

[6] T. Hu, M. Hu, Z. Li, H. Zhang, C. Zhang, J. Wang, X. Wang, Interlayer coupling in two-dimensional titanium carbide MXenes, Phys. Chem. Chem. Phys. 18 (2016) 20256–20260. https://doi.org/10.1039/C6CP01699E.

[7] Y. Gogotsi, B. Anasori, The Rise of MXenes, ACS Nano 13 (2019) 8491–8494. https://doi.org/10.1021/acsnano.9b06394.

[8] D. Zhang, M. Ashton, A. Ostadhossein, A.C.T. van Duin, R.G. Hennig, S.B. Sinnott, Computational Study of Low Interlayer Friction in Tin+1Cn (n = 1, 2, and 3) MXene, ACS Appl. Mater. Interfaces 9 (2017) 34467–34479. https://doi.org/10.1021/acsami.7b09895.

[9] C. Donnet, A. Erdemir, Solid Lubricant Coatings: Recent Developments and Future Trends, Tribol Lett 17 (2004) 389–397. https://doi.org/10.1023/B:TRIL.0000044487.32514.1d.

[10] C. Donnet, A. Erdemir, Historical developments and new trends in tribological and solid lubricant coatings, Surf. Coat. Technol. 180-181 (2004) 76–84. https://doi.org/10.1016/j.surfcoat.2003.10.022.

[11] T.W. Scharf, S.V. Prasad, Solid lubricants: a review, J Mater Sci 48 (2013) 511–531. https://doi.org/10.1007/s10853-012-7038-2.

[12] S. Rao, M. Sandeep, R. Kumaraswami, A. Shravan, A critical review on solid lubricants, International Journal of Mechanical Engineering and Technology 7 (2016) 193–199.

[13] S.H. Wan, Solid Lubricant: Soft Metal, in: Q.J. Wang, Y.-W. Chung (Eds.), Encyclopedia of Tribology, Springer US, Boston, MA, 2013, pp. 3152–3159.

[14] M.R. Vazirisereshk, A. Martini, D.A. Strubbe, M.Z. Baykara, Solid Lubrication with MoS2: A Review, Lubricants 7 (2019) 57. https://doi.org/10.3390/lubricants7070057.

[15] H.S. Khare, D.L. Burris, The Effects of Environmental Water and Oxygen on the Temperature-Dependent Friction of Sputtered Molybdenum Disulfide, Tribol Lett 52 (2013) 485–493. https://doi.org/10.1007/s11249-013-0233-8.

[16] B. Vierneusel, T. Schneider, S. Tremmel, S. Wartzack, T. Gradt, Humidity resistant MoS2 coatings deposited by unbalanced magnetron sputtering, Surf. Coat. Technol. 235 (2013) 97–107. https://doi.org/10.1016/j.surfcoat.2013.07.019.

[17] A. Mesgarnejad, M.M. Khonsari, On the tribological behavior of MoS2-coated thrust ball bearings operating under oscillating motion, Wear 269 (2010) 547–556. https://doi.org/10.1016/j.wear.2010.05.010.

[18] H. Singh, K.C. Mutyala, H. Mohseni, T.W. Scharf, R.D. Evans, G.L. Doll, Tribological Performance and Coating Characteristics of Sputter-Deposited Ti-Doped MoS 2 in Rolling and Sliding Contact, Tribol. Trans. 58 (2015) 767–777. https://doi.org/10.1080/10402004.2015.1015758.

[19] D. Berman, A. Erdemir, A.V. Sumant, Graphene: a new emerging lubricant, Materials Today 17 (2014) 31–42. https://doi.org/10.1016/j.mattod.2013.12.003.

[20] F. Pape, G. Poll, Investigations on Graphene Platelets as Dry Lubricant and as Grease Additive for Sliding Contacts and Rolling Bearing Application, Lubricants 8 (2020) 3. https://doi.org/10.3390/lubricants8010003.

[21] C. Donnet, A. Erdemir, Tribology of Diamond-Like Carbon Films: Fundamentals and Applications, Springer, Boston, 2008.

[22] A.W. Zia, Z. Zhou, L.K.-Y. Li, Structural, mechanical, and tribological characteristics of diamond-like carbon coatings, in: Nanomaterials-Based Coatings, Elsevier, 2019, pp. 171–194.

[23] J. Kröner, S. Kursawe, Y. Musayev, S. Tremmel, Analysing the Tribological Behaviour of DLC-Coated Dry-Running Deep Groove Ball Bearings with Regard to the Ball Material, AMM 856 (2016) 143–150. https://doi.org/10.4028/www.scientific.net/AMM.856.143.

[24] J. Kröner, S. Tremmel, S. Wartzack, Untersuchungen an a-C:H:Me-beschichteten Rillenkugellagern unter Trockenlaufbedingungen, Tribologie und Schmierungstechnik 66 (2019) 33–39. https://doi.org/10.30419/TuS-2019-0030.

[25] A. Vanhulsel, F. Velasco, R. Jacobs, L. Eersels, D. Havermans, E.W. Roberts, I. Sherrington, M.J. Anderson, L. Gaillard, DLC solid lubricant coatings on ball bearings for space applications, Tribol. Int. 40 (2007) 1186–1194. https://doi.org/10.1016/j.triboint.2006.12.005.

[26] A. Rosenkranz, Y. Liu, L. Yang, L. Chen, 2D nano-materials beyond graphene: from synthesis to tribological studies, Appl Nanosci 10 (2020) 3353–3388. https://doi.org/10.1007/s13204-020-01466-z.

[27] M. Malaki, R.S. Varma, Mechanotribological Aspects of MXene-Reinforced Nanocomposites, Adv. Mater. Weinheim. 32 (2020) e2003154. https://doi.org/10.1002/adma.202003154.

[28] J. Yang, B. Chen, H. Song, H. Tang, C. Li, Synthesis, characterization, and tribological properties of two-dimensional Ti 3 C 2, Crystal Research and Technology 49 (2014) 926–932. https://doi.org/10.1002/crat.201400268.

[29] Y. Liu, X. Zhang, S. Dong, Z. Ye, Y. Wei, Synthesis and tribological property of Ti3C2TXnanosheets, Journal of Materials Science 52 (2017) 2200–2209. https://doi.org/10.1007/s10853-016-0509-0.

[30] X. Zhang, Y. Guo, Y. Li, Y. Liu, S. Dong, Preparation and tribological properties of potassium titanate-Ti3C2Tx nanocomposites as additives in base oil, Chinese Chemical Letters 30 (2019) 502–504. https://doi.org/10.1016/j.cclet.2018.07.007.

[31] M. Xue, Z. Wang, F. Yuan, X. Zhang, W. Wei, H. Tang, C. Li, Preparation of TiO 2 /Ti 3 C 2 T x hybrid nanocomposites and their tribological properties as base oil lubricant additives, RSC Adv. 7 (2017) 4312–4319. https://doi.org/10.1039/C6RA27653A.

[32] J. Hu, S. Li, J. Zhang, Q. Chang, W. Yu, Y. Zhou, Mechanical properties and frictional resistance of Al composites reinforced with Ti3C2T MXene, Chinese Chemical Letters 31 (2020) 996–999. https://doi.org/10.1016/j.cclet.2019.09.004.

[33] Y.J. Mai, Y.G. Li, S.L. Li, L.Y. Zhang, C.S. Liu, X.H. Jie, Self-lubricating Ti3C2 nanosheets/copper composite coatings, Journal of Alloys and Compounds 770 (2019) 1–5. https://doi.org/10.1016/j.jallcom.2018.08.100.

[34] H. Zhang, L. Wang, Q. Chen, P. Li, A. Zhou, X. Cao, Q. Hu, Preparation, mechanical and anti-friction performance of MXene/polymer composites, Materials & Design 92 (2016) 682–689. https://doi.org/10.1016/j.matdes.2015.12.084.

[35] H. Zhang, L. Wang, A. Zhou, C. Shen, Y. Dai, F. Liu, J. Chen, P. Li, Q. Hu, Effects of 2-D transition metal carbide Ti 2 CT x on properties of epoxy composites, RSC Adv. 6 (2016) 87341–87352. https://doi.org/10.1039/C6RA14560D.

[36] W. Lian, Y. Mai, C. Liu, L. Zhang, S. Li, X. Jie, Two-dimensional Ti3C2 coating as an emerging protective solid-lubricant for tribology, Ceramics International 44 (2018) 20154–20162. https://doi.org/10.1016/j.ceramint.2018.07.309.

[37] A. Rosenkranz, P.G. Grützmacher, R. Espinoza, V.M. Fuenzalida, E. Blanco, N. Escalona, F.J. Gracia, R. Villarroel, L. Guo, R. Kang, F. Mücklich, S. Suarez, Z. Zhang, Multi-layer Ti3C2Tx-nanoparticles (MXenes) as solid lubricants – Role of surface terminations and intercalated water, Appl. Surf. Sci. 494 (2019) 13–21. https://doi.org/10.1016/j.apsusc.2019.07.171.

[38] Y. Guo, X. Zhou, D. Wang, X. Xu, Q. Xu, Nanomechanical Properties of Ti3C2 Mxene, Langmuir 35 (2019) 14481–14485. https://doi.org/10.1021/acs.langmuir.9b02619.

[39] X. Zhou, Y. Guo, D. Wang, Q. Xu, Nano friction and adhesion properties on Ti3C2 and Nb2C MXene studied by AFM, Tribol. Int. 153 (2021) 106646. https://doi.org/10.1016/j.triboint.2020.106646.

[40] A. Rodriguez, M.S. Jaman, O. Acikgoz, B. Wang, J. Yu, P.G. Grützmacher, A. Rosenkranz, M.Z. Baykara, The potential of Ti3C2TX nano-sheets (MXenes) for nanoscale solid lubrication revealed by friction force microscopy, Appl. Surf. Sci. 535 (2021) 147664. https://doi.org/10.1016/j.apsusc.2020.147664.

[41] M. Marian, G.C. Song, B. Wang, V.M. Fuenzalida, S. Krauß, B. Merle, S. Tremmel, S. Wartzack, J. Yu, A. Rosenkranz, Effective usage of 2D MXene nanosheets as solid lubricant – Influence of contact pressure and relative humidity, Appl. Surf. Sci. 531 (2020) 147311. https://doi.org/10.1016/j.apsusc.2020.147311.

[42] X. Yin, J. Jin, X. Chen, A. Rosenkranz, J. Luo, Ultra-Wear-Resistant MXene-Based Composite Coating via in Situ Formed Nanostructured Tribofilm, ACS Appl. Mater. Interfaces 11 (2019) 32569–32576. https://doi.org/10.1021/acsami.9b11449.

[43] X. Yin, J. Jin, X. Chen, A. Rosenkranz, J. Luo, Interfacial Nanostructure of 2D Ti 3 C 2 /Graphene QDs Hybrid Multicoating for Ultralow Wear, Adv. Eng. Mater. (2020). https://doi.org/10.1002/adem.201901369.

[44] H. Yan, L. Zhang, H. Li, X. Fan, M. Zhu, Towards high-performance additive of Ti3C2/graphene hybrid with a novel wrapping structure in epoxy coating, Carbon 157 (2020) 217–233. https://doi.org/10.1016/j.carbon.2019.10.034.

[45] P.G. Grützmacher, S. Suarez, A. Tolosa, C. Gachot, G. Song, B. Wang, V. Presser, F. Mücklich, B. Anasori, A. Rosenkranz, Superior Wear-Resistance of Ti3C2Tx Multilayer Coatings, ACS Nano (2021). https://doi.org/10.1021/acsnano.1c01555.

[46] H. Singh, K.C. Mutyala, R.D. Evans, G.L. Doll, An investigation of material and tribological properties of Sb2O3/Au-doped MoS2 solid lubricant films under sliding and rolling contact in different environments, Surf. Coat. Technol. 284 (2015) 281–289. https://doi.org/10.1016/j.surfcoat.2015.05.049.

[47] M. Marian, S. Tremmel, S. Wartzack, G. Song, B. Wang, J. Yu, A. Rosenkranz, MXene nanosheets as an emerging solid lubricant for machine elements – Towards increased energy efficiency and service life, Appl. Surf. Sci. 523 (2020) 1–8. https://doi.org/10.1016/j.apsusc.2020.146503.

[48] ISO, 104:2015-09 Rolling bearings - Thrust bearings - Boundary dimensions, general plan.

[49] X. Shi, T.W. Liskiewicz, B.D. Beake, Z. Sun, J. Chen, Fretting wear behavior of graphite-like carbon films with bias-graded deposition, Appl. Surf. Sci. 494 (2019) 929–940. https://doi.org/10.1016/j.apsusc.2019.07.265.

[50] X. Shi, T.W. Liskiewicz, B.D. Beake, J. Chen, C. Wang, Tribological performance of graphite-like carbon films with varied thickness, Tribol. Int. 149 (2020) 105586. https://doi.org/10.1016/j.triboint.2019.01.045.

[51] J. Kröner, S. Tremmel, S. Kursawe, Y. Musayev, T. Hosenfeldt, S. Wartzack, GreenBearings – Friction Behaviour of DLC-Coated Dry Running Deep Groove Ball Bearings, AMM 805 (2015) 147–153. https://doi.org/10.4028/www.scientific.net/AMM.805.147.

[52] A. Seynstahl, S. Krauß, E. Bitzek, B. Meyer, B. Merle, S. Tremmel, Microstructure, Mechanical Properties and Tribological Behavior of Magnetron-Sputtered MoS2 Solid Lubricant Coatings Deposited under Industrial Conditions, Coatings 11 (2021) 455. https://doi.org/10.3390/coatings11040455.

[53] B. Vierneusel, L. Benker, S. Tremmel, M. Göken, B. Merle, Isolating the effect of residual stresses on coating wear by a mechanical stress relaxation technique, International Conference on Metallurgical Coatings, San Diego, 1989 638 (2017) 159–166. https://doi.org/10.1016/j.tsf.2017.06.016.

[54] E.I. Preiß, B. Merle, Y. Xiao, F. Gannott, J.P. Liebig, J.M. Wheeler, M. Göken, Applicability of focused Ion beam (FIB) milling with gallium, neon, and xenon to the fracture toughness characterization of gold thin films, J. Mater. Res. (2021). https://doi.org/10.1557/s43578-020-00045-w.

[55] B. Rothammer, K. Neusser, M. Marian, M. Bartz, S. Krauß, T. Böhm, S. Thiele, B. Merle, R. Detsch, S. Wartzack, Amorphous Carbon Coatings for Total Knee Replacements-Part I: Deposition,

Cytocompatibility, Chemical and Mechanical Properties, Polymers 13 (2021). https://doi.org/10.3390/polym13121952.

[56] A.C. Ferrari, J. Robertson, Raman spectroscopy of amorphous, nanostructured, diamond-like carbon, and nanodiamond, Philos. Trans. A Math. Phys. Eng. Sci. 362 (2004) 2477–2512. https://doi.org/10.1098/rsta.2004.1452.

[57] W.G. Cui, Q.B. Lai, L. Zhang, F.M. Wang, Quantitative measurements of sp3 content in DLC films with Raman spectroscopy, Surf. Coat. Technol. 205 (2010) 1995–1999. https://doi.org/10.1016/j.surfcoat.2010.08.093.

[58] F.C. Tai, S.C. Lee, C.H. Wei, S.L. Tyan, Correlation between I_D/I_G Ratio from Visible Raman Spectra and sp^2/sp^3 Ratio from XPS Spectra of Annealed Hydrogenated DLC Film, Mater. Trans. 47 (2006) 1847–1852. https://doi.org/10.2320/matertrans.47.1847.

[59] Y. Wang, H. Li, L. Ji, F. Zhao, Q. Kong, Y. Wang, X. Liu, W. Quan, H. Zhou, J. Chen, Microstructure, mechanical and tribological properties of graphite-like amorphous carbon films prepared by unbalanced magnetron sputtering, Surf. Coat. Technol. 205 (2011) 3058–3065. https://doi.org/10.1016/j.surfcoat.2010.11.019.

[60] D.N. Khaemba, A. Neville, A. Morina, A methodology for Raman characterisation of MoDTC tribofilms and its application in investigating the influence of surface chemistry on friction performance of MoDTC lubricants, Tribol Lett 59 (2015). https://doi.org/10.1007/s11249-015-0566-6.

[61] T.J. Wieting, Long-wavelength lattice vibrations of MoS2 and GaSe, Solid State Communications 12 (1973) 931–935. https://doi.org/10.1016/0038-1098(73)90111-7.

[62] B.C. Windom, W.G. Sawyer, D.W. Hahn, A Raman Spectroscopic Study of MoS2 and MoO3: Applications to Tribological Systems, Tribol Lett 42 (2011) 301–310. https://doi.org/10.1007/s11249-011-9774-x.

[63] S. Domínguez-Meister, T.C. Rojas, M. Brizuela, J.C. Sánchez-López, Solid lubricant behavior of MoS2 and WSe2-based nanocomposite coatings, Sci. Technol. Adv. Mater. 18 (2017) 122–133. https://doi.org/10.1080/14686996.2016.1275784.

[64] J.J. Hu, R. Wheeler, J.S. Zabinski, P.A. Shade, A. Shiveley, A.A. Voevodin, Transmission Electron Microscopy Analysis of Mo–W–S–Se Film Sliding Contact Obtained by Using Focused Ion Beam Microscope and In Situ Microtribometer, Tribol Lett 32 (2008) 49–57. https://doi.org/10.1007/s11249-008-9360-z.

[65] J.M. Chen, C.S. Wang, Second order Raman spectrum of MoS2, Solid State Communications 14 (1974) 857–860. https://doi.org/10.1016/0038-1098(74)90150-1.

[66] G.L. Frey, R. Tenne, M.J. Matthews, M.S. Dresselhaus, G. Dresselhaus, Raman and resonance Raman investigation of MoS2 nanoparticles, Phys. Rev. B 60 (1999) 2883–2892. https://doi.org/10.1103/PhysRevB.60.2883.

[67] M. Hu, T. Hu, Z. Li, Y. Yang, R. Cheng, J. Yang, C. Cui, X. Wang, Surface Functional Groups and Interlayer Water Determine the Electrochemical Capacitance of Ti3C2 T x MXene, ACS Nano 12 (2018) 3578–3586. https://doi.org/10.1021/acsnano.8b00676.

[68] T. Hu, J. Wang, H. Zhang, Z. Li, M. Hu, X. Wang, Vibrational properties of Ti3C2 and Ti3C2T2 (T = O, F, OH) monosheets by first-principles calculations: a comparative study, Phys. Chem. Chem. Phys. 17 (2015) 9997–10003. https://doi.org/10.1039/C4CP05666C.

[69] X. Zhang, Y. Liu, S. Dong, Z. Ye, Y. Guo, One-step hydrothermal synthesis of a TiO2-Ti3C2Tx nanocomposite with small sized TiO2 nanoparticles, Ceramics International 43 (2017) 11065–11070. https://doi.org/10.1016/j.ceramint.2017.05.151.

[70] A. Sarycheva, Y. Gogotsi, Raman Spectroscopy Analysis of the Structure and Surface Chemistry of Ti 3 C 2 T x MXene, Chem. Mater. 32 (2020) 3480–3488. https://doi.org/10.1021/acs.chemmater.0c00359.

[71] V. Buck, Structure and density of sputtered MoS2-films, Vacuum 36 (1986) 89–94. https://doi.org/10.1016/0042-207X(86)90277-0.

[72] A. LiBassi, A.C. Ferrari, V. Stolojan, B.K. Tanner, J. Robertson, L.M. Brown, Density, sp 3 content and internal layering of DLC films by X-ray reflectivity and electron energy loss spectroscopy, Diamond and Related Materials 9 (2000) 771–776. https://doi.org/10.1016/S0925-9635(99)00233-2.

[73] D.K. Avasthi, D. Kabiraj, Jaipal, G.K. Mehta, H.C. Barshilia, S. Sah, B.R. Mehta, v.d. Vankar, Study of hydrogen in DLC film by ERDA with 58Ni ions, Vacuum 46 (1995) 633–636. https://doi.org/10.1016/0042-207X(95)00004-6.

[74] B. Vierneusel, Verschleiß- und feuchteresistente MoS2-Festschmierstoffschichten für den Gleit- und Wälzkontakt: Reihe 1, Konstruktionstechnik, Maschinenelemente, Nr. 440, Fortschritt-Berichte VDI, Düsseldorf, 2017.

[75] Y. Wang, J. Li, L. Shan, J. Chen, Q. Xue, Tribological performances of the graphite-like carbon films deposited with different target powers in ambient air and distilled water, Tribol. Int. 73 (2014) 17–24. https://doi.org/10.1016/j.triboint.2013.12.022.

[76] S.K. Field, M. Jarratt, D.G. Teer, Tribological properties of graphite-like and diamond-like carbon coatings, Tribol. Int. 37 (2004) 949–956. https://doi.org/10.1016/j.triboint.2004.07.012.

[77] S.-C. Shi, J.-Y. Wu, Y.-Q. Peng, Transfer layer formation in MoS2/hydroxypropyl methylcellulose composite, Wear 408-409 (2018) 208–213. https://doi.org/10.1016/j.wear.2018.05.019.

[78] Z. Chen, X. He, C. Xiao, S. Kim, Effect of Humidity on Friction and Wear—A Critical Review, Lubricants 6 (2018) 74. https://doi.org/10.3390/lubricants6030074.

[79] L. Wang, L. Bai, Z. Lu, G. Zhang, Z. Wu, Influence of Load on the Tribological Behavior of a-C Films: Experiment and Calculation Coupling, Tribol Lett 52 (2013) 469–475. https://doi.org/10.1007/s11249-013-0230-y.

[80] R. Christy, Sputtered MoS2 lubricant coating improvements, Thin Solid Films 73 (1980) 299–307. https://doi.org/10.1016/0040-6090(80)90493-9.

[81] M. Nishimura, M. Suzuki, Solid-lubricated ball bearings for use in a vacuum — state-of-the-art, Tribol. Int. 32 (1999) 637–647. https://doi.org/10.1016/S0301-679X(99)00089-4.